Supporting Information

Visible-Light-Driven Photoelectrocatalytic Degradation of Tetracycline Using Dual Z-Scheme Bi_2MoO_6/GQDs/TiO_2 Heterojunctions

Feiyu Li, Kailu Liu, Hanyue Zhang, Xing Wang, Jingui Ma, Yansheng Liu and Junwei Hou

State Key Laboratory of Heavy Oil Processing, China University of Petroleum (Beijing) at Karamay, Karamay, Xinjiang 834000, China

This part includes 7 figures.

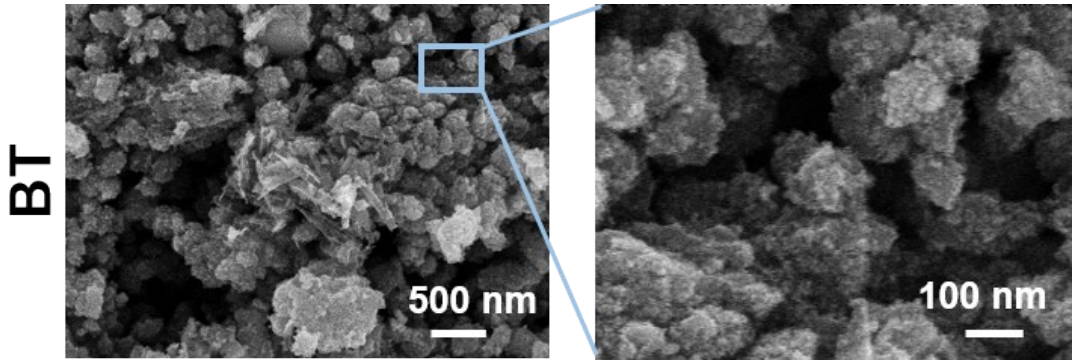

Figure S1. SEM images of BT.

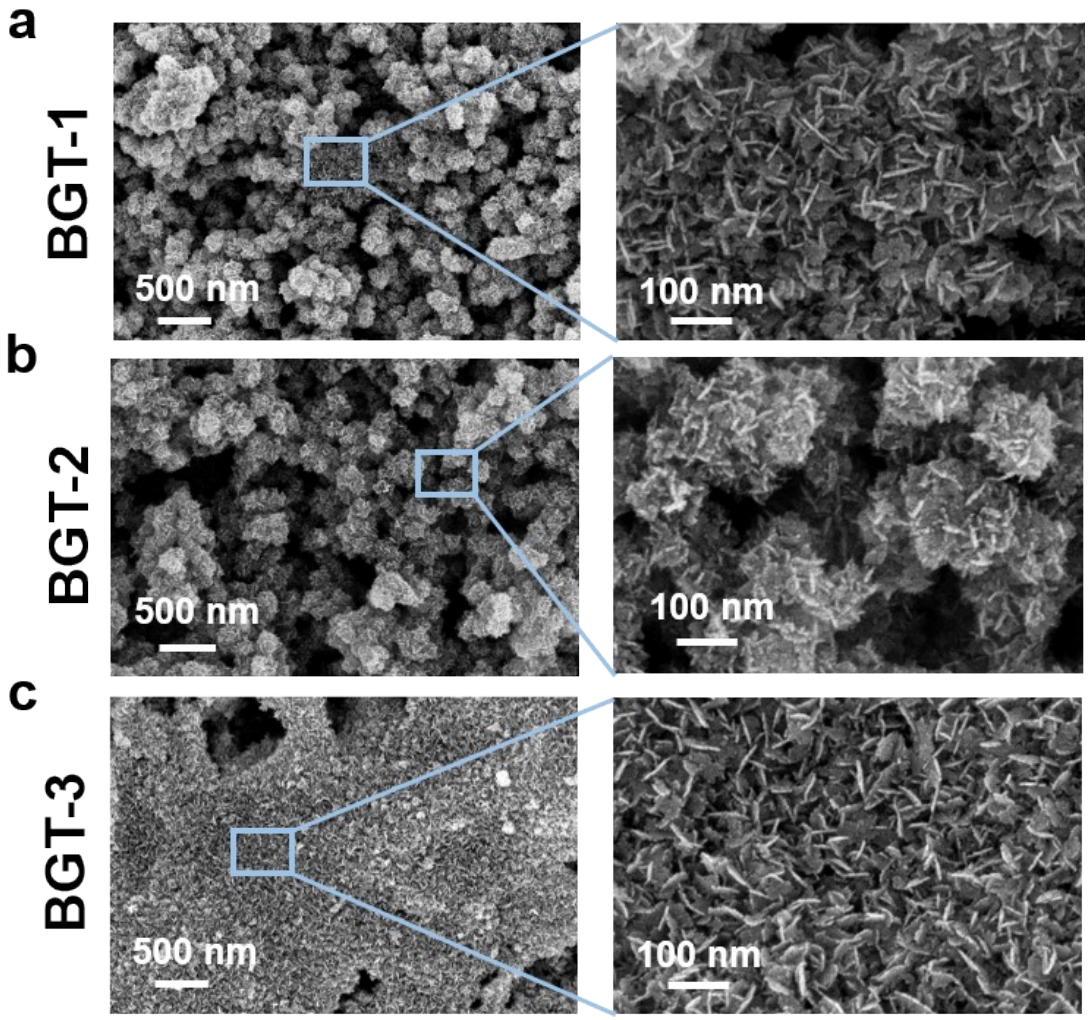

Figure S2. SEM images of (a) BGT1, (b) BGT-2 and (c) BGT-3 with different GQDs concentrations.

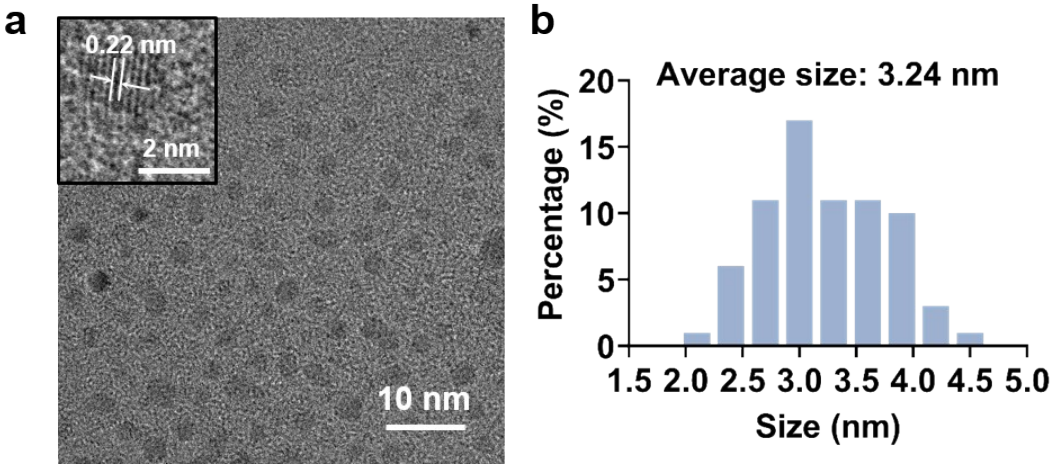

Figure S3. (a) TEM images and (b) the size distribution of GQDs.

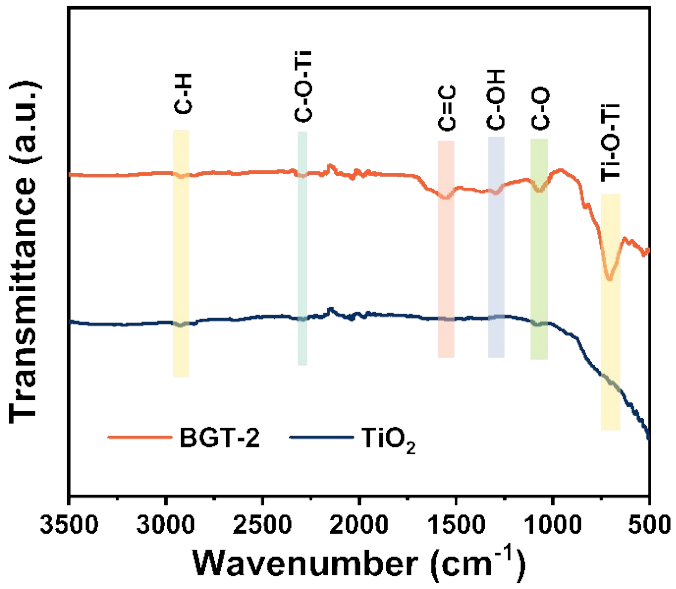

Figure S4. FTIR spectra of TiO_2 and BGT-2.

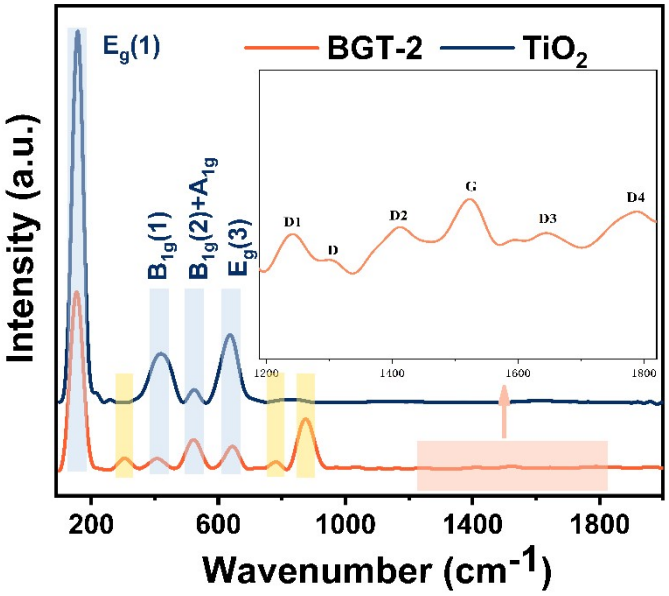

Figure S5. Raman spectra of TiO_2 and BGT-2.

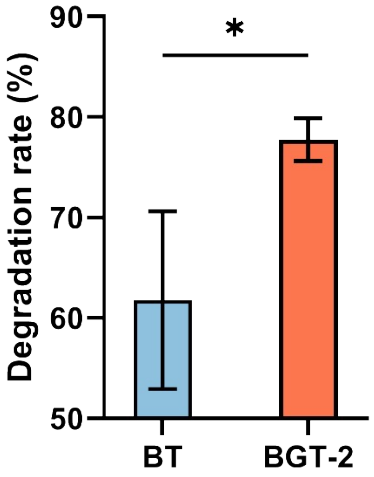

Figure S6. Statistical significance analysis of degradation rates by BGT-2 and BT photocatalyst. Statistical significance was analyzed via the two-tailed Student's t-test (***$p < 0.001$, **$p < 0.01$, and *$p < 0.05$).（n=5）

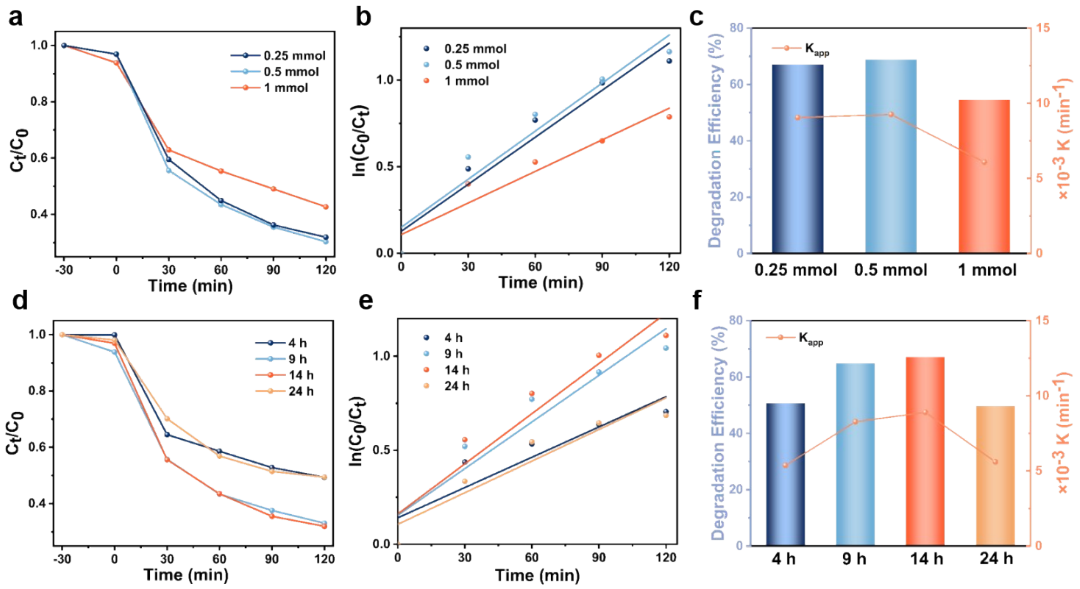

Figure S7. (a) Time-dependent photodegradation curves, (b) kinetic curves, and (c) degradation efficiency and rate constants for TC of BGT materials with different hydrothermal times. (d) Time-dependent photodegradation curves, (e) kinetic curves, and (f) degradation efficiency and rate constants for TC of BGT materials with different Bi_2MoO_6 contents

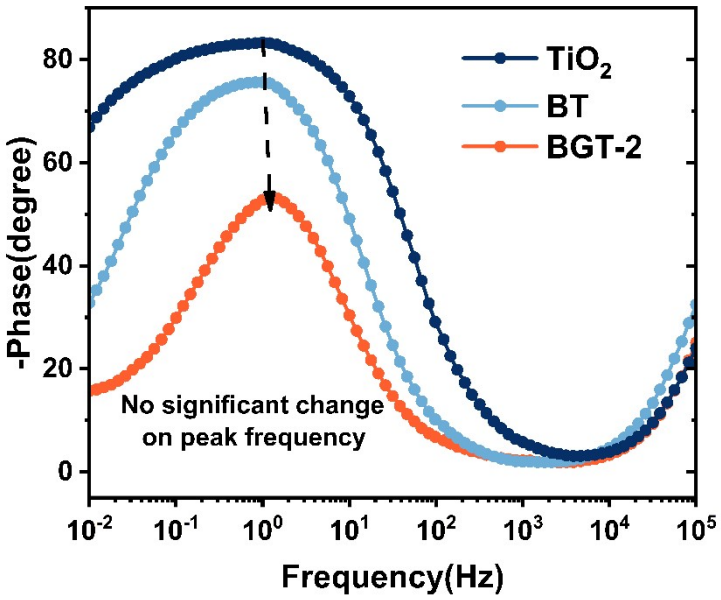

Figure S8. Bode plots of TiO_2, BT, and BGT-2.

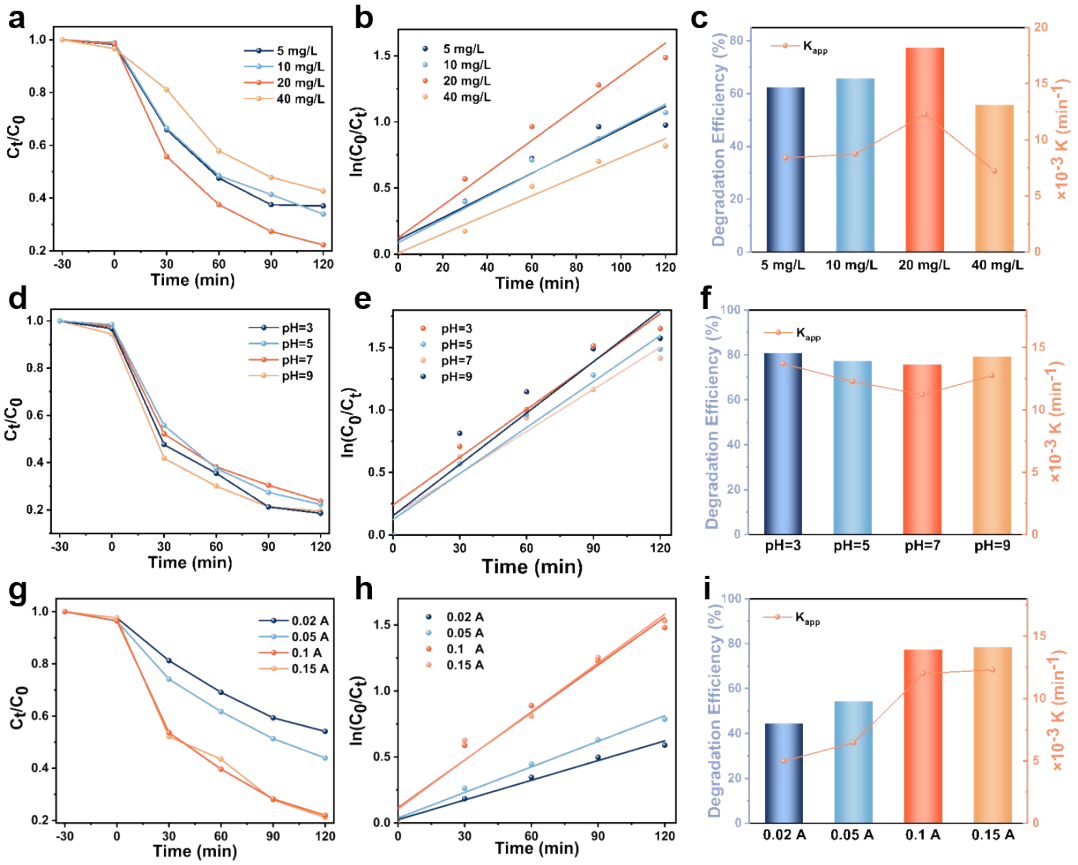

Figure S9. Time-dependent PEC degradation curves, kinetic curves, and degradation efficiency and rate constants for TC degradation of BGT-2 under different (a-c) initial concentration of TC, (d-f) pH value, and (g-i) applied current.

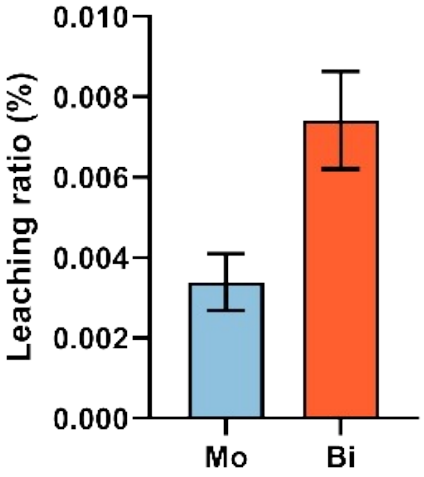

Figure S10. Ratio of Mo/Bi leaching after PEC process. (n=5)